IJASRM
International Journal of Advanced Scientific Research and Management, Volume 9 Issue 1, Jan 2024

www.ijasrm.com

ISSN 2455-6378

Design and Analysis of a Car Body Using Aerodynamic Model

Dr. K. Manigandan[1]

[1] Department of Mechanical Engineering, Podhigai College of Engineering and Technology, Tirupattur, Tamil Nadu 635601, India

Abstract

Aerodynamics plays a vital role in the design process of automobiles. It significantly impacts the vehicle's fuel economy by reducing wind resistance in the form of drag force. The focus of this study is specifically on the side surface of cars and aims to demonstrate how implementing tapered top views and rear-end boat-tailed contours can effectively decrease drag. Aerodynamic analysis was performed on diverse three-dimensional designs featuring increasing camber and varying side configurations. Utilizing Computational Fluid Dynamics tools, the curvatures specified in each design were manipulated to achieve the minimum drag coefficient. This study aimed to identify optimal design options that would result in a fuel-efficient and aerodynamically streamlined car. Ultimately, this research has the potential to contribute towards the development of a vehicle with enhanced fuel economy and reduced fuel consumption. The pressure distribution results have been used to determine the coefficient of drag, drag force, and percentage of fuel consumption caused by drag. With a modification of the camber up to 200 mm, the drag force can be effectively reduced from 480 N to 400 N at a top speed of 30 m/s. Moreover, by curving the sides of the car, there is also a significant decrease in the percentage of fuel consumption attributed to drag force, with a reduction of 5% observed at 30 m/s.

Keywords: *Aerodynamic, Car design, Fuel economy, Drag force, Coefficient drag force, Velocity*

1. Introduction

Recently, the automotive industry requires the technology to develop a vehicle body that possesses high strength, high rigidity, and lightweight properties. This necessity arises from the industry's aim to enhance crashworthiness and reduce CO_2 emissions. However, the industry now faces a critical need to produce lighter vehicles due to the growing demand for reduced fuel consumption. This demand is driven by the need to combat global warming, oil-resource depletion, and other environmental problems [1]. To achieve this, automotive manufacturers must implement measures to minimize aerodynamic drag, which is crucial for improving fuel economy. It is worth noting that aerodynamic drag at high speeds accounts for the majority of a vehicle's running resistance. While the vehicle body incorporates comprehensive measures to minimize aerodynamic drag, it also boasts attractive styling and enables efficient packaging [2]. The combination of superior aerodynamic efficiency, packaging and styling stands as one of the most significant attributes in vehicle development.

Aerodynamics is the study of the motion of air and the resulting forces acting on solids in relation to such fluid. The flow of fluid over a moving vehicle can be categorized into three types: The flow within the vehicle's machinery, the flow of air through the vehicle, the flow of air around the vehicle. Therefore, vehicle aerodynamics focuses on the vehicle's shape, its impact on the moving vehicle, the examination of air and its response to the surrounding flow field during motion [4]. The primary components of aerodynamic effects include lift, side wind, drag, rolling moment, pitching moment, yawing moment.

When fluid flows over a body, a net resultant force is exerted on the vehicle. The drag force, which is the component of the resultant force parallel to the flow direction, opposes the vehicle's motion and must be overcome by the engine's power. Consequently, the drag force directly impacts the vehicle's performance and fuel economy [5]. Additionally, the pressure difference between the upper and lower surfaces of the vehicle generates a resultant force perpendicular to the direction of motion, known as lift. Lift acts in an upward direction and affects the effective tire

https://doi.org/10.36282/IJASRM/9.1.2024.1923

International Journal of Advanced Scientific Research and Management, Volume 9 Issue 1, Jan 2024

IJASRM

www.ijasrm.com

ISSN 2455-6378

loads. In the presence of crosswinds, the flow may become asymmetrical. This leads to areas of negative pressure on the forward lee side edge and in the region of the A-pillar, while a slightly positive pressure is observed on the windward side. At the rear end, there is a zone of slightly low pressure on the lee side compared to the windward side. Consequently, the asymmetrical pressure distribution gives rise to lateral forces and yawing moments [7].

Furthermore, a pitching moment is present in addition to lift, with respect to the lateral axis. This pitching moment arises from the disparity in lift forces between the fore body and after body of a vehicle. A reference point, situated on the road at the center of the wheelbase and track, is crucial for calculating this pitching moment. Additionally, in asymmetric flow conditions such as crosswinds, a moment with respect to the vertical axis may also arise [2]. The force that causes a turning motion in a vehicle is known as the yawing moment. It has been observed that this moment increases with changes in wind direction. The yawing moment is directly linked to the wheelbase of the vehicle and can steer it away from the wind [8]. In situations where there are uneven air flows, such as crosswinds, a rolling moment is created along the longitudinal center axis. This phenomenon has a minor impact on directional stability and its importance is influenced by the roll steering capabilities of the chassis.

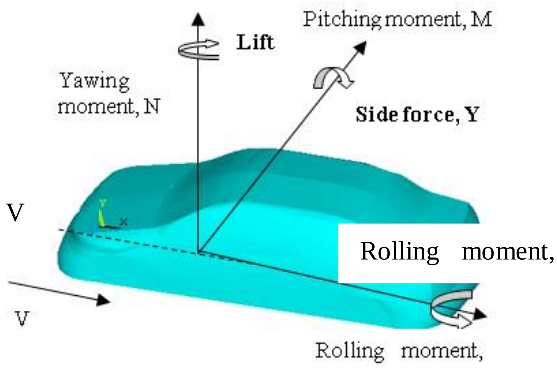

Fig.1 Forces and moments acting on a vehicle

2. Aerodynamic Testing Procedure

Computational Fluid Dynamics (CFD) has been utilized by the automotive industry to complement their wind tunnel testing, reducing the need for extensive planning and cost of the maintenance and operation and enabling faster design cycles. The application of CFD involves the utilization of the continuity equation, the Energy equation, navier-Stokes equations and a turbulence model [7]. In this particular study, the focus is on implementing a styling concept to redesign the top view tapered and rear end boat tailed contours of a sports utility vehicle. This redesign aims to further decrease the drag coefficient, where the current design features a straight line. In this study, models of varying dimensions ranging from 0 to 200 mm were utilized for the analysis. The computational model includes FLUID 142 (Flotran element) as its element type. The fluid environment surrounding the car was enlarged three times bigger than the standard dimensions of the car [5]. In formulating the problem, several assumptions were made such as fixing the reference temperature to 293 K and setting the standard atmospheric pressure of 1.013 bar as a reference value of 0 bar. ANSYS software was also used for computational fluid dynamic analysis. Through using Pro/E software the initial model's dimensions were varied to achieve aero-styling in the design process.. Based on these results, a fuel efficient and aerodynamically stylized model was designed Dimensions of the car is shown in figure 2 [9].

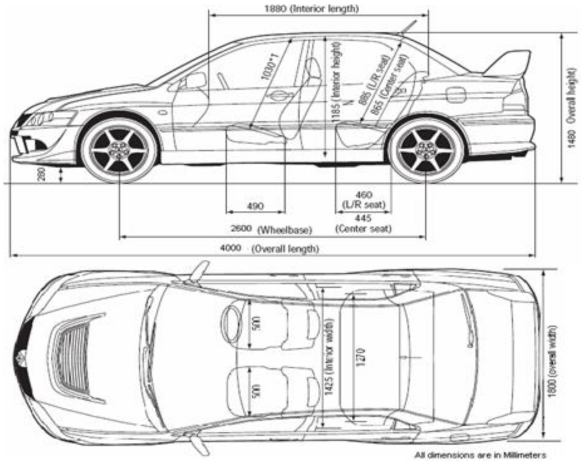

Fig.2 Dimensions of the car

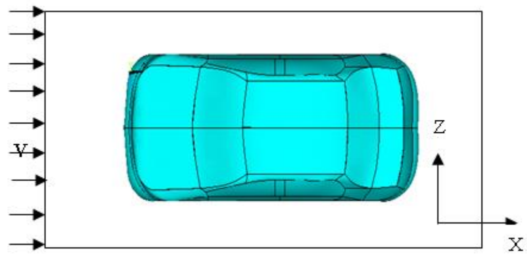

Fig. 3 Physical description of computational domain

Physical description of computational domain is shown in figure 3. It is assumed that there is only one phase in the fluid and that the analysis will be either turbulent or laminar, depending on user input. In addition, the user must determine whether to use the incompressible algorithm or the compressible algorithm [11]. The boundary conditions include gradually increasing velocity from 5 to 30 m/s at the inlet, with a turbulent intensity of 1% as shown in

https://doi.org/10.36282/IJASRM/9.1.2024.1923

International Journal of Advanced Scientific Research and Management, Volume 9 Issue 1, Jan 2024

IJASRM

www.ijasrm.com

ISSN 2455-6378

figure 4. At the outlet, there is a zero gradient along the main flow direction and standard atmospheric pressure is applied to exit boundary face. The bottom, left, top and sides of the computational area are considered walls, with a velocity constraint of zero on any surfaces touching the car based on boundary layer calculations [10].

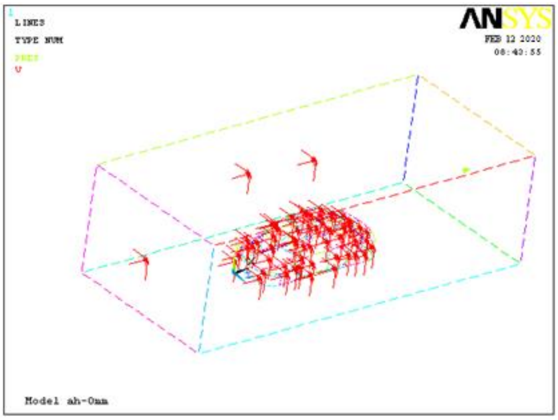

Fig. 4 Applied boundary conditions

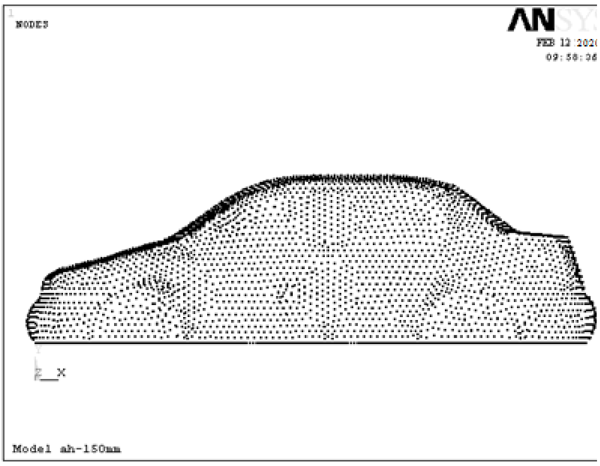

Fig. 5 Nodes attached to the surface of the car

3. Results and Discussions

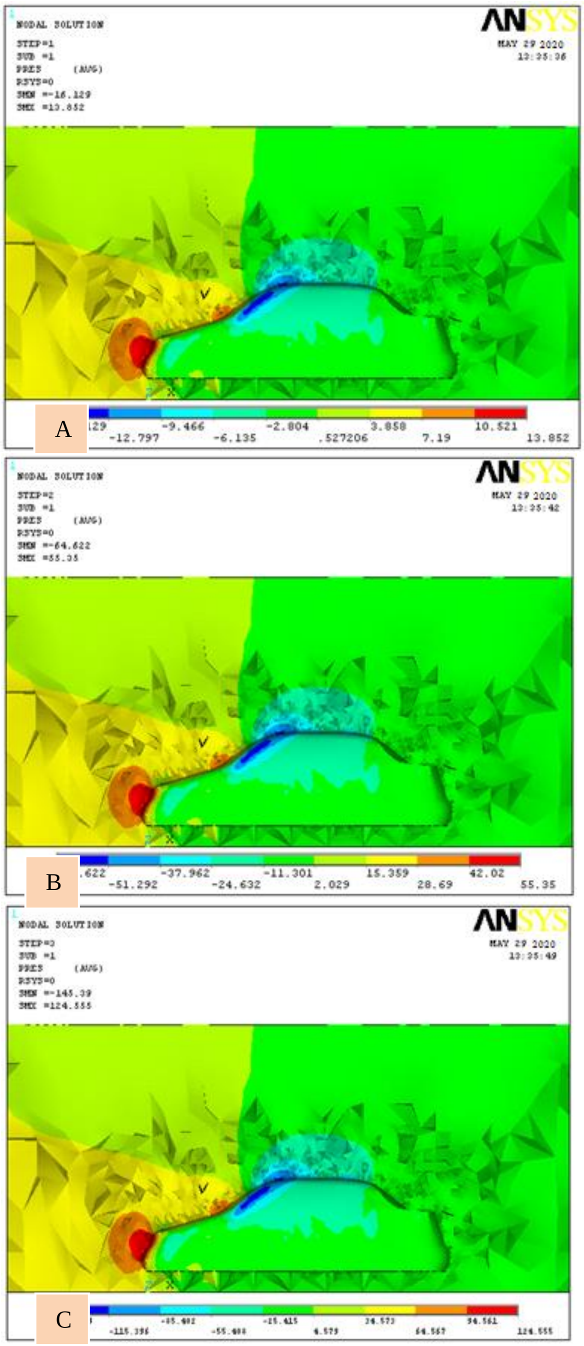

https://doi.org/10.36282/IJASRM/9.1.2024.1923

International Journal of Advanced Scientific Research and Management, Volume 9 Issue 1, Jan 2024

IJASRM

www.ijasrm.com

ISSN 2455-6378

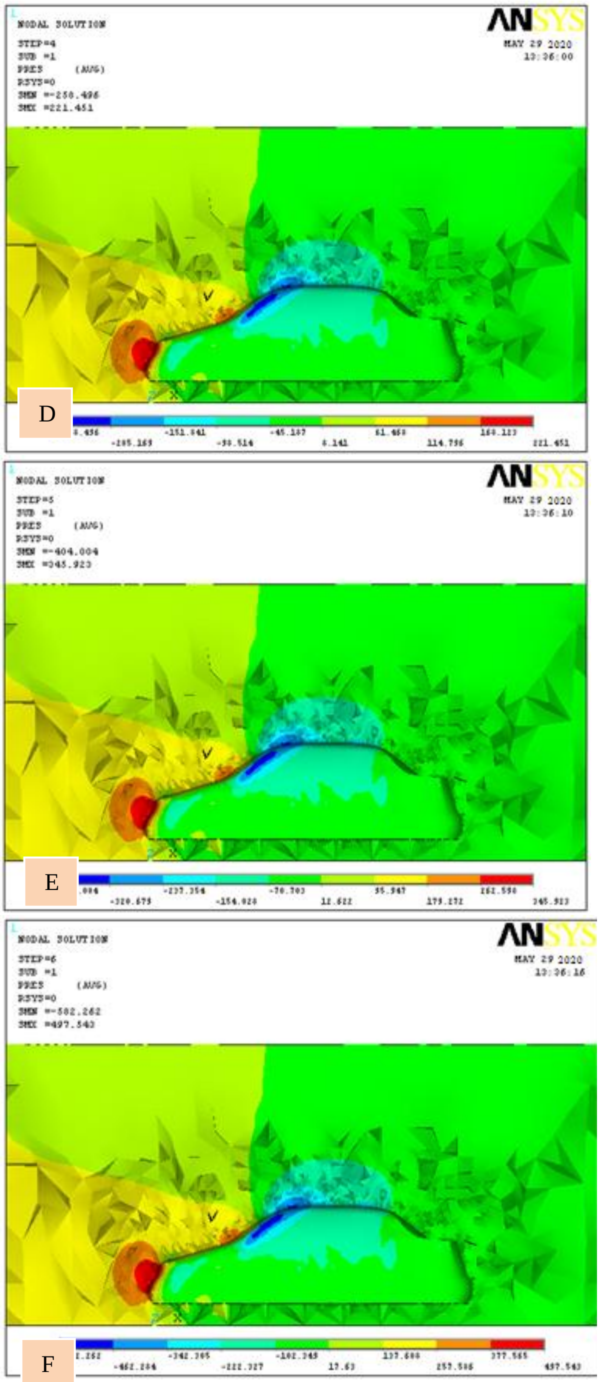

Fig. 6 Pressure distributions for MODEL-E (200 mm) at different velocities in 5, 10, 15, 20, 25, 30 m/s respectively

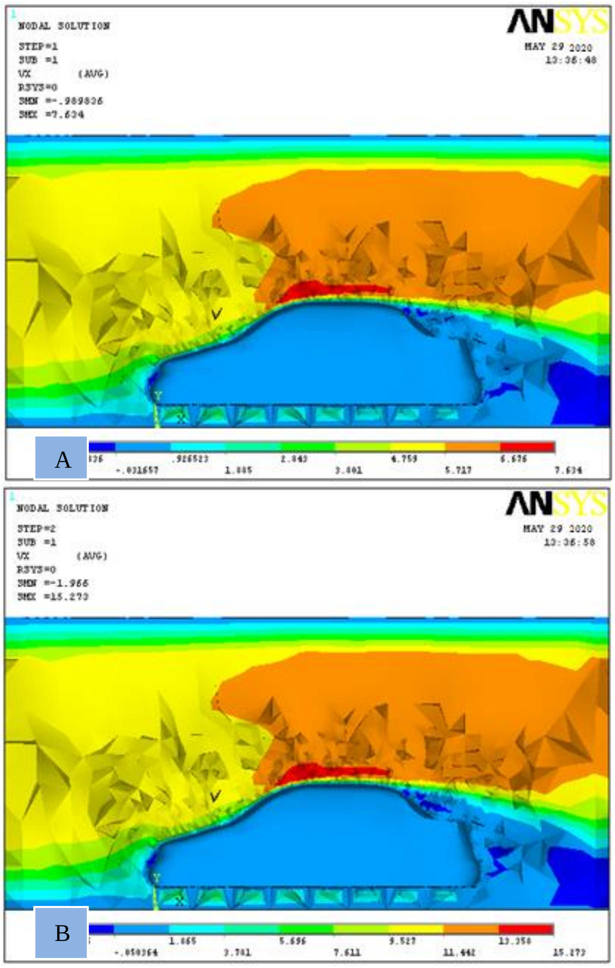

https://doi.org/10.36282/IJASRM/9.1.2024.1923

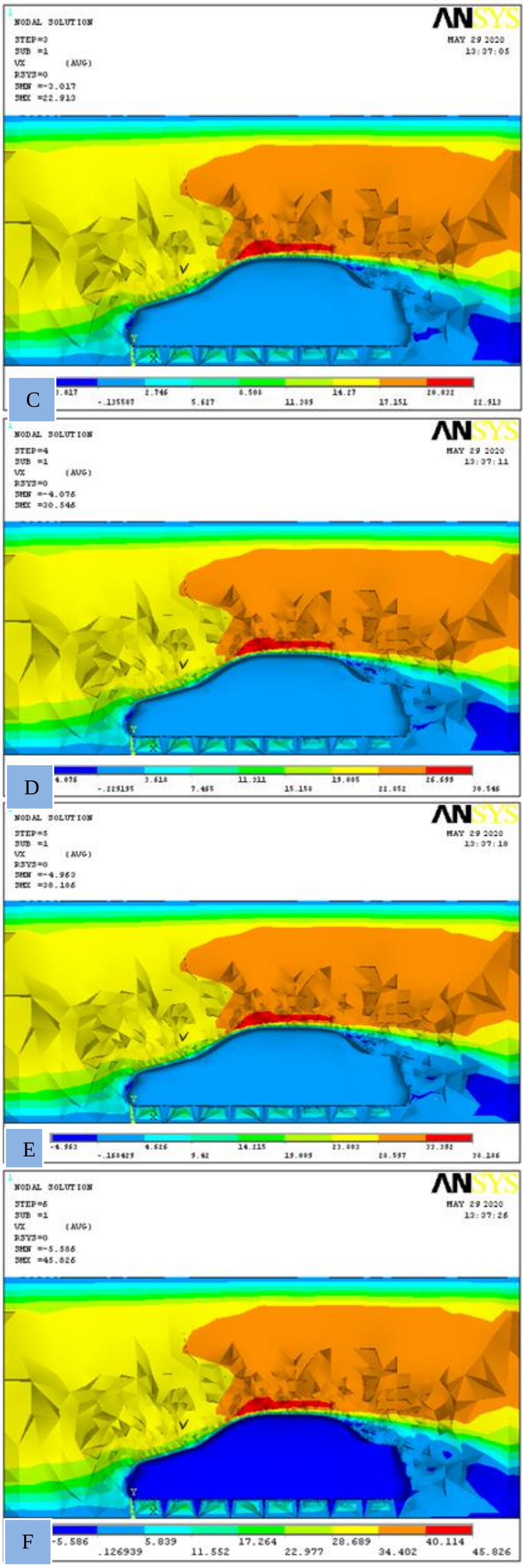

Fig. 7 Velocity distributions (Vx) for MODEL-E (200 mm) at different velocities in m/s 5, 10, 15, 20, 25, 30 m/s respectively

Sample Calculations for the Car Model-A at 30 m/s

Average pressure at the back of the car (p_b) $= -p_b \times (1+\sin\beta)/2$

$= -40.39\times(1+0.573)/2$

$= -31.77\ N/m^2$

Average pressure at the front of the car

$= (p1+p2\sin\alpha+p2\sin\delta+p3\sin\alpha+p3\sin\delta+p4\sin\delta)/6$

$=(543.81+(417.96+292.105)\times0.728+166.24\times0.453)/6$

$= 190.92\ N/m^2$

Drag force (D) $= \dfrac{C_D\,\rho A V^2}{2}$

$= \dfrac{[0.41\times1.2\times2.16\times30^2]}{2}$

$= 481.04$ N

Pressure drag coefficient (C_D) $= \dfrac{\text{Static pressure}}{\text{Dynamic pressure}}$

$= [p_f - p_b] / \rho V^2/2$

$= [190.92-(-31.77)]/[(1.2\times30^2)(1/2)]$

$= 0.41.$

Rolling resistance (R_R) $= r_o\times m\times g$

$= 0.015\times1410\times9.81$

$= 207.48$ N

Total Resistance $= R_R + D$

$= 207.48+481.04$

$= 688.52$ N

$$\frac{[\text{Liters / kilometers}]_{\text{Drag}}}{[\text{Liters / kilometers}]} = \frac{D}{[D+R_R]}$$

$= 481.04/[481.04+207.48]$

$= 0.69 = 69\%$

https://doi.org/10.36282/IJASRM/9.1.2024.1923

The sample calculations for calculating the fuel drag force and total resistance at the velocity of 30 m/s is given above. For different models of the car Drag force (D), drag coefficient (C_D) and fuel consumption rate with varying cambers are predicted based on calculations. The comparisons are plotted in a graph and the calculation results are listed in table 1. It is observed that from the calculations the coefficient of drag is minimized from 0.42 to 0.34 with camber of 200 mm (MODEL E) at the sides of the car as shown in figure 8. At different velocities for the individual models the required drag force are determined and tabulated below [12].

Table 1 Coefficient of Drag (C_D) for the models at different velocities

Models of the Car	Cambers	Coefficient of Drag at Different Velocities					
		30	25	20	15	10	5
A-Model	0 mm	0.41	0.41	0.41	0.41	0.41	0.41
B-Model	50 mm	0.40	0.40	0.40	0.41	0.40	0.40
C-Model	100 mm	0.41	0.41	0.40	0.40	0.40	0.40
D-Model	150 mm	0.35	0.35	0.35	0.36	0.35	0.32
E-Model	200 mm	0.34	0.34	0.34	0.34	0.34	0.34

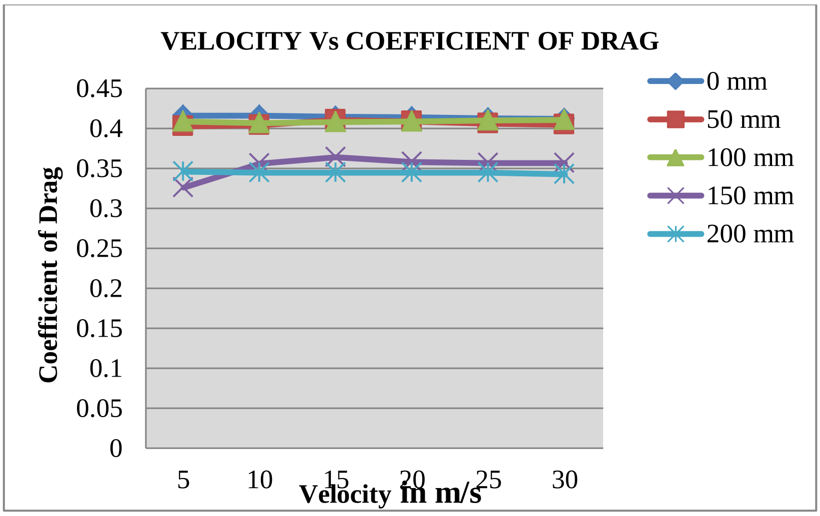

Fig. 8 Coefficient of drag for different car models

https://doi.org/10.36282/IJASRM/9.1.2024.1923

IJASRM
International Journal of Advanced Scientific Research and Management, Volume 9 Issue 1, Jan 2024
www.ijasrm.com
ISSN 2455-6378

Table 2 Drag force (D) for the models at different velocities

Models of the Car	Cambers	Drag Force at Different Velocities (M/S)					
		30	25	20	15	10	5
A-Model	0 mm	481.04	334.68	214.75	121.23	54.01	13.49
B-Model	50 mm	472.81	329.02	212.40	120.00	52.46	13.08
C-Model	100 mm	479.90	332.61	212.22	119.21	52.82	13.26
D-Model	150 mm	416.45	289.87	186.07	106.28	46.23	10.56
E-Model	200 mm	401.03	279.56	179.09	110.73	44.75	11.23

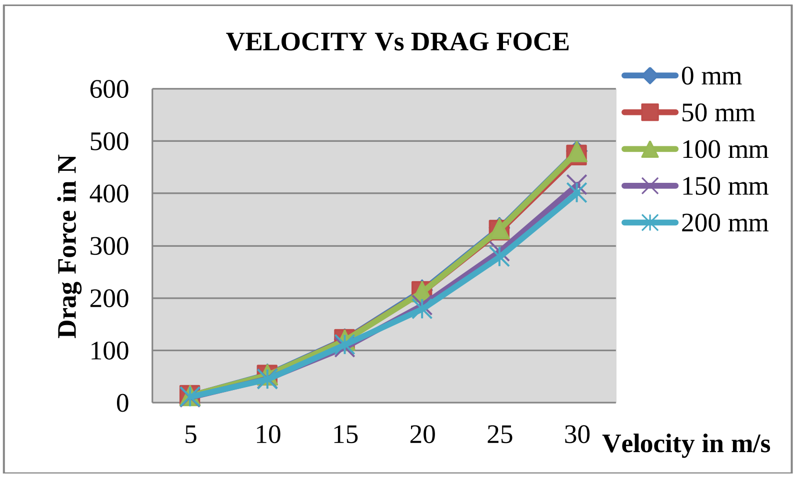

Fig. 9 Aerodynamic Drag force for different car models

Table 3 Percentage of fuel consumption for the models at different velocities

Models of the Car	Camber	Percentage of Fuel Consumption at Different Velocities (M/S)					
		30	25	20	15	10	5
A-Model	0 mm	69.00	61.73	50.86	36.88	20.65	6.1
B-Model	50 mm	77.29	61.32	50.58	36.64	20.18	5.9
C-Model	100 mm	77.41	61.58	50.26	36.49	20.29	6
D-Model	150 mm	73.29	58.28	47.28	33.87	18.22	4.8
E-Model	200 mm	72.22	57.4	46.32	34.79	17.74	5.1

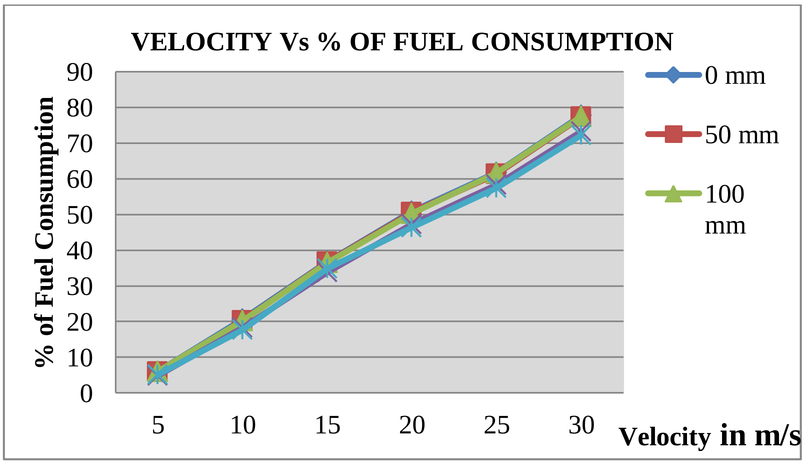

Fig. 10 Aerodynamic drag force for different car models

https://doi.org/10.36282/IJASRM/9.1.2024.1923

From figure 9 it is clearly observed that by raising the vehicle speed the car model's drag force is slowly increased. The drag force is decreased by 16% by considering camber of 200 mm. it is clearly defined that from the figure 10 the percentage of fuel consumption gradually reduces by providing camber to the vehicle car model. The drag force is reduced by 5% by providing 200 mm camber. The velocity and pressure distributions for MODEL-E for various velocities are shown in figure 6 and 7 respectively, which cause less fuel consumptions and drag force.

4. Conclusions

From the analysis of different models, it is addressed that the coefficient of drag for the models gradually reduces by providing the camber at sides of the car.

1. The change in drag coefficient is in the order of 0.01. From the drag coefficient the drag force for different models are calculated and the percentage reduction in drag force is around 16%.
2. The coefficient of drag is reduced from 0.42 to 0.34 when the camber increased from 0 mm to 200 mm.
3. The fuel consumption is decreased 5% by providing the camber. The engine overcoming the percentage of fuel consumption by the drag force is determined.

References

[1] ANSYS release 10.0 theoretical references manual.

[2] Alessandro Talamelli, Johan Westin, Mekanik/KTH, "*Vehicle Aerodynamics Introduction", power point presentation*.

[3] Michael Zabat, Nick Stabile And Frederick Browand (1995),"The Aerodynamic Performance Of Platoons: Final Report", California Path research report, *Institute of Transportation Studies, University of California*, Berkeley, ISSN 1055- 1425.

[4] Sun Yongling, Wu Guangqiang and Xieshuo, "Numerical Simulation of the External Flow Field around A Bluff Car", *Automotive Engineering Department*, Shanghai Tongji University, Shanghai, China.

[5] Wolf-Heinrieh Hucho (1998),"Aerodynamics of road vehicles", fourth edition, *SAE Inc*, 1998.

[6] Mitsubishi lancer evolution VIII, *Mitsubishi Motors, Japan Press Information*, Jan. 2003.

[7] Norbert Grüin (1996), "Simulating External Vehicle Aerodynamics with Cart Low", *SAE transaction*, 960679.

[8] Mats Ramnefors, Rikard Bensryd, Elna Holmberg and Sven Perzon (1996), "Accuracy of Drag Predictions on Cars Using CFD- Effect of Grid Refinement and Turbulence Models", *SAE transaction*, 960681.

[9] Toshio Kobayashi and Kozo Kitsh (1992), "A Review of CFD Methods and Their Application to Automobile Aerodynamics", *SAE transaction*, 920338.

[10] Masaru Koike Tsunehisa Nagayoshi Naoki Hamamoto (2004) "Research on Aerodynamic Drag Reduction by Vortex Generator Technical review" 2004 No.16, *Mitsubishi Motors*.

[11] Subrata Roy and Pradeep Srinivasan "External Flow Analysis of a Truck for Drag Reduction", *SAE transaction*, 2000-01-3500.

[12] Inchul Kim And Xin Geng, "Optimization of Body shapes through Computation of Aerodynamic Forces on Low Mass Vehicle", Department Of Mechanical Engineering, *University Of Michigan- Dearborn*, Dearborn, MI 48128.

https://doi.org/10.36282/IJASRM/9.1.2024.1923